

## Article

# Coagulation Combined with Electro-Fe<sup>0</sup>/H<sub>2</sub>O<sub>2</sub> Reaction for Effective Treatment of Landfill Leachate Effluent of Membrane Bioreactor

Cheng Long <sup>1</sup>, Bin Zhu <sup>1,2,3,\*</sup>, Wei Liu <sup>3</sup> and Qixuan Li <sup>3</sup><sup>1</sup> School of Environment and Energy, South China University of Technology, Guangzhou 510006, China<sup>2</sup> Analysis and Testing Center, South China University of Technology, Guangzhou 510640, China<sup>3</sup> Guangdong Zihua Technology Limited Company, Foshan 528000, China

\* Correspondence: esbzhu@scut.edu.cn; Tel.: +86-138-0290-7271

**Abstract:** In this study, coagulation combined with the electro-Fe<sup>0</sup>/H<sub>2</sub>O<sub>2</sub> reaction was developed to treat refractory organics in the landfill leachate effluent of a membrane bioreactor (MBR), and the change in biodegradability was investigated. The results showed that polymerized ferric sulfate (PFS) was the best coagulant, with removal efficiencies of chemical oxygen demand (COD) and chromaticity of 74.18% and 72.22%, respectively, when the dosage was 2 g/L and the initial pH (pH<sub>0</sub>) was 6. Under the optimal conditions of pH<sub>0</sub> of 3, current density of 5 mA/cm<sup>2</sup>, Fe<sup>0</sup> dosage of 3 g/L, and H<sub>2</sub>O<sub>2</sub> dosage of 0.059 M, the electro-Fe<sup>0</sup>/H<sub>2</sub>O<sub>2</sub> reaction showed the removal efficiencies of COD and chromaticity for coagulated effluent were 76.68% and 74%, respectively. UV-vis and 3D-EEM spectral analysis showed that humic and fulvic acids were effectively degraded, and the effluent was mostly small molecules of aromatic protein-like substances. The whole process increased the BOD<sub>5</sub>/COD from 0.049 to 0.46, indicating that the biodegradability was substantially improved. This is due to the conjunction of the Fe<sup>0</sup>/H<sub>2</sub>O<sub>2</sub> reaction with electrochemistry, which accelerated the reduction of Fe<sup>3+</sup> to Fe<sup>2+</sup> on the Fe<sup>0</sup> surface and cathode and improved the efficiency of hydroxyl radical (•OH) generation, thus promoting the removal of pollutants. The operating cost was only 4.18 \$/m<sup>3</sup>, with the benefits of less Fe<sup>0</sup> loss and no pH adjustment. In summary, coagulation combined with the electro-Fe<sup>0</sup>/H<sub>2</sub>O<sub>2</sub> reaction is a cost-effective method for treating refractory organics in leachate and enhancing biodegradability.



**Citation:** Long, C.; Zhu, B.; Liu, W.; Li, Q. Coagulation Combined with Electro-Fe<sup>0</sup>/H<sub>2</sub>O<sub>2</sub> Reaction for Effective Treatment of Landfill Leachate Effluent of Membrane Bioreactor. *Water* **2023**, *15*, 1158. <https://doi.org/10.3390/w15061158>

Academic Editor: Antonio Zuorro

Received: 23 February 2023

Revised: 11 March 2023

Accepted: 15 March 2023

Published: 16 March 2023



**Copyright:** © 2023 by the authors. Licensee MDPI, Basel, Switzerland. This article is an open access article distributed under the terms and conditions of the Creative Commons Attribution (CC BY) license (<https://creativecommons.org/licenses/by/4.0/>).

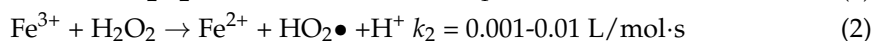
**Keywords:** zero-valent iron; fenton reaction; coagulation; landfill leachate; biodegradability

## 1. Introduction

Landfill leachate is a type of wastewater containing high concentrations of organic pollutants such as ammonia, salts, heavy metals, and other organic compounds (such as pesticides) due to the decomposition of solid waste and infiltration of rainfall [1,2]. Since landfill leachate is toxic and complex in composition, posing a significant threat to water resources and human health, it should not be discharged into the environment untreated [3,4]. Biological treatment is being used extensively for landfill leachate initial stage treatment due to its efficiency in degrading bio-available chemicals (such as phenols as well as heterocyclic and acyclic compounds) and its high cost-effective advantages [5,6]. Membrane bioreactor (MBR) technology, a more advanced biological treatment process, can further reduce COD, ammonia nitrogen, and organic micropollutants (such as endocrine disruptors (EDCs)) in landfill leachate, with the advantages of a small footprint and high efficiency [7,8]. However, the MBR effluent still contains a large amount of refractory organic contaminants such as humic and fulvic acids, causing a high COD (500–4000 mg/L) and low biodegradability (BOD<sub>5</sub>/COD < 0.1), which is unable to meet the discharge standard [8]. Therefore, a process is urgently needed to treat leachate MBR effluent in depth and improve its biodegradability.

Different technologies, such as coagulation [9], adsorption [10], advanced oxidation techniques (AOPs) [11], nanofiltration, and reverse osmosis [12], are widely used for the deep treatment of leachate. In recent years, coagulation combined with AOPs has been considered an effective method of depth treatment of leachate for the removal of refractory organic matter [9,13]. Coagulation is often used as a pretreatment step of the AOPs method because treating leachate with AOPs alone is too expensive. The coagulation mechanism is mainly to neutralize the negatively charged refractory organics (e.g., humic acid) so that the unstable particles agglomerate and form larger and heavier flocs [14]. However, the disadvantage of coagulation is its inability to completely remove and mineralize the organic contaminants in leachate [15].

AOPs are considered a viable technology for the treatment of refractory organic contaminants in landfill leachate [9]. The Fenton method, a commonly used AOP, is widely used for the removal of organic contaminants from leachate [16–18]. In this process, hydrogen peroxide is catalyzed by  $\text{Fe}^{2+}$  to produce hydroxyl radicals ( $\bullet\text{OH}$ ), the radicals of  $\bullet\text{OH}$  have a high reduction potential of 2.8 V and the ability to decompose most refractory organic contaminants to  $\text{CO}_2$ ,  $\text{H}_2\text{O}$ , or intermediate products such as organic acids [6]. These intermediate products are in biodegradable forms, and the biodegradability of leachate is enhanced [19]. The Fenton chain reaction is shown in Equations (1) and (2) [20].



Equations (1) and (2) produce a  $\text{Fe}^{3+}/\text{Fe}^{2+}$  cyclic reaction that helps maintain the  $\text{Fe}^{2+}$  concentration. However, since  $k_2$  is rather insignificant compared to  $k_1$ , it is difficult for the traditional Fenton method to regenerate  $\text{Fe}^{2+}$ , so a large amount of  $\text{Fe}^{3+}$  is accumulated in the reaction system, resulting in a considerable amount of iron sludge after the reaction [6,21]. To solve this problem,  $\text{Fe}^0$  powder is used as an alternative iron source to the conventional Fenton reaction and combined with electrochemistry.  $\text{Fe}^0$  corrosion produces  $\text{Fe}^{2+}$  in situ, and the  $\text{Fe}^{2+}$  production pathway is shown in Equation (3) [22]. The generated  $\text{Fe}^{2+}$  further catalyzes  $\text{H}_2\text{O}_2$  to produce  $\bullet\text{OH}$ . In addition, due to the presence of  $\text{Fe}^0$  and current,  $\text{Fe}^{3+}$  was converted to  $\text{Fe}^{2+}$  on the surface of  $\text{Fe}^0$  and the cathode, which avoids the accumulation of  $\text{Fe}^{3+}$  and reduces the production of iron hydroxide after the reaction, as shown in Equations (4) and (5) [22–25]. This enables a more efficient decomposition of  $\text{H}_2\text{O}_2$  into hydroxyl radicals in the system and enhances the oxidation capacity of the system.



Recently, the  $\text{Fe}^0/\text{H}_2\text{O}_2$  reaction has been widely used in wastewater, including rhodamine B (RhB) [26], landfill leachate [27,28], salty wastewater [29], and phenol wastewater [30]. Fenton processes combined with electrochemistry are also widely applied in dye and landfill leachate due to their eco-friendly advantages [20,31,32]. Moreover, the electro-Fenton process, with a sacrificial anode catalyzing the Fenton reaction, is also widely used in the treatment of wastewater [33]. However, few studies have combined the  $\text{Fe}^0/\text{H}_2\text{O}_2$  reaction with electrochemistry for improving leachate biodegradability. In addition, by combining coagulation with an electro- $\text{Fe}^0/\text{H}_2\text{O}_2$  reaction, the coagulated effluent can proceed to the next treatment step without pH adjustment, which saves the cost of chemicals. The electro- $\text{Fe}^0/\text{H}_2\text{O}_2$  reaction deeply removes the refractory organics and improves the biodegradability of the leachate, which helps subsequent standard discharge treatment (aerobic biological treatment).

In this study, coagulation combined with the electro- $\text{Fe}^0/\text{H}_2\text{O}_2$  reaction was developed to treat landfill leachate MBR effluent. The removal efficiency of the whole process on COD and chromaticity were investigated. UV-vis spectra and a three-dimensional excitation and emission matrix (3D-EEM) were used to analyze the transformation direction of refractory

organic pollutants in leachate and to assess changes in biodegradability. Additionally, the operating cost of coagulation combined with the electro-Fe<sup>0</sup>/H<sub>2</sub>O<sub>2</sub> reaction was evaluated.

## 2. Materials and Methods

### 2.1. Leachate and Material

The landfill leachate is the effluent treated by the A-O/A-O-MBR process and collected from a landfill in Guangzhou, Guangdong Province, China. To prevent further biodegradation, the leachate was placed in a polypropylene bucket and kept at 4 °C. The characteristics of leachate are listed in Table 1.

**Table 1.** Characteristics of the leachate.

Parameters	Value
COD (mg/L)	3378.5
BOD5 (mg/L)	166.3
BOD5/COD	0.049
pH	7.2
Chromaticity (times)	1800

Polymethyl methacrylate was used to construct the electrolytic cell, which measured 8 cm × 7 cm × 12 cm. A Ti/IrO<sub>2</sub>-RuO<sub>2</sub>-TiO<sub>2</sub> anode and a Ti cathode, both 10 cm × 5 cm in size, with a 7 cm × 5 cm immersing part and a 35 cm<sup>2</sup> working area, were placed parallel to each other at a 5 cm distance. Use an electric mixer with the speed set to 120 rpm to evenly distribute the Fe<sup>0</sup> powder inside the cell. The electrodes were connected to a DC power supply (MS-155D, MAISHENG Company, Guangzhou, China) with a voltage range of 0–15 V and a current range of 0–5 A. The experimental device is shown in Figure 1.

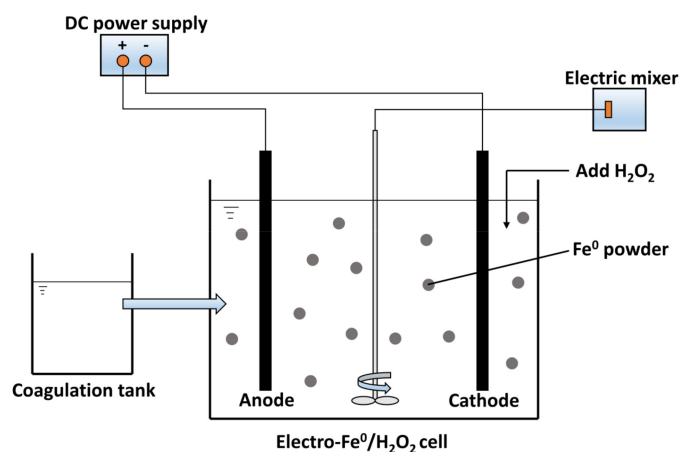


**Figure 1.** The experimental device of coagulation combined with the electro-Fe<sup>0</sup>/H<sub>2</sub>O<sub>2</sub> reaction.

### 2.2. Chemicals

Polymerized ferric sulfate (PFS), polymerized aluminum chloride (PAC), and aluminum sulfate (Al<sub>2</sub>(SO<sub>4</sub>)<sub>3</sub>) were purchased from Tianjin Damao Chemical Reagent Factory (Tianjin, China), and hydrogen peroxide (30% w/w) was purchased from Chengdu Kolong Chemical Co. (Chengdu, China). Fe<sup>0</sup> was a powder with a particle size of 0.05 mm. Other conventional agents such as NaOH, H<sub>2</sub>SO<sub>4</sub>, and polyacrylamide (PAM) were analytical grade and purchased from the Guangzhou Chemical Reagent Factory (Guangzhou, China).

### 2.3. Experimental Procedure

#### 2.3.1. Coagulation Process

PAC, PFS, and Al<sub>2</sub>(SO<sub>4</sub>)<sub>3</sub> (AS) were selected as coagulants. The optimal coagulants and dosage for the treatment of leachate were investigated. Firstly, 200 mL of leachate

was placed in a 250 mL beaker. Then it was injected with different doses of coagulant and specific PAM. The beaker was then immediately placed on a magnetic stirrer and stirred uniformly for 10 min, left to settle for 30 min, and the supernatant was taken for COD and chromaticity analysis. Under the conditions of the best coagulant and the best dosage, the pH was adjusted with 1M H<sub>2</sub>SO<sub>4</sub> and NaOH to investigate the effect of pH<sub>0</sub> on the coagulation effect. The sedimentation performance of the sludge was evaluated using the sludge settling velocity (SV<sub>30min</sub>) at different pH<sub>0</sub>. Under optimal coagulation conditions, the coagulated effluent is used in the subsequent electro-Fe<sup>0</sup>/H<sub>2</sub>O<sub>2</sub> reaction.

### 2.3.2. Electro-Fe<sup>0</sup>/H<sub>2</sub>O<sub>2</sub> Reaction

First, the 500 mL of coagulated effluent was discharged into the cell, and the pH<sub>0</sub> was adjusted with 1 M H<sub>2</sub>SO<sub>4</sub> and NaOH if necessary. Fe<sup>0</sup> powder and hydrogen peroxide were added to the cell while electricity was applied. An electric mixer was used to make the Fe<sup>0</sup> powder evenly dispersed in the solution at 120 rpm. Samples were taken at regular intervals within a certain time range, and the samples were immediately adjusted to pH 8 and left to settle for one hour, followed by a centrifuge for 5 min at 5000 rpm (to separate the sludge). The supernatant was taken for analysis of COD and chromaticity. The pH<sub>0</sub>, current density, Fe<sup>0</sup> powder dosage, and hydrogen peroxide dosage were varied to determine the optimal electro-Fe<sup>0</sup>/H<sub>2</sub>O<sub>2</sub> conditions.

### 2.4. Analytical Methods

The concentrations of COD and BOD<sub>5</sub> during the experiments were determined according to the standard methods [34]. The pH value was measured with a HACH Pocket Pro<sup>+</sup> pH tester (HACH Co., Loveland, CO, USA). The chromaticity is measured with a colorimeter (SD9011B, Xinrui Instrument Co., Shanghai, China).

The UV-vis spectra were scanned with an ultraviolet spectrophotometer (Agilent Cary 60) in the wavelength range of 230 to 450 nm at 24,000 nm/min with a scanning interval of 5 nm. The 3D-EEM was recorded with a fluorescence spectrophotometer (F-7000, Hitachi, Japan). Excitation and emission were scanned simultaneously in the wavelength ranges of 200 to 450 nm and 250 to 550 nm, respectively, both with a slit width of 5 nm and a scanning speed of 1200 nm/min. The fluorescence regional integration (FRI) was used to analyze the fluorescence intensity data in 3D-EEM.

## 3. Results and Discussion

### 3.1. Coagulation Process

According to previous studies, the type and dose of coagulant are crucial for the removal of organic matter [9]. Therefore, this experiment investigated the removal efficiency of COD and the chromaticity of leachate with different coagulants and dosages.

As shown in Figure 2a,b, the removal efficiency of PFS for COD and the chromaticity of MBR effluent increased between 1.0 and 2.0 g/L with the dosage. The highest removal efficiencies of PFS for COD and chromaticity were 73.36% and 71.67%, respectively, at the dosage of 2 g/L. The removal efficiency of PAC for COD and chromaticity increased with the increase in dosage, and the highest removal rate was achieved at 3.5–4 g/L and remained stable at about 68%, while the removal efficiency of AS for COD and chromaticity was lower at about 38% and 45%, respectively, and the removal efficiency was almost unaffected by the change in dosage. Since the comprehensive performance of PFS is better than that of PAC and AS, PFS is chosen as the coagulant. When the amount of PFS is low, the coagulation of colloids in solution is mainly through the electric neutralization of the coagulant. At this time, the concentration of iron in solution is not enough to completely neutralize the negative charge on the surface of colloids, and the coagulation effect is poor. When an excessive amount of PFS was added, an inhibition phenomenon occurred due to the repulsive force between polymeric coagulants, and the excessive amount of PFS would prevent the aggregation of colloids [35].

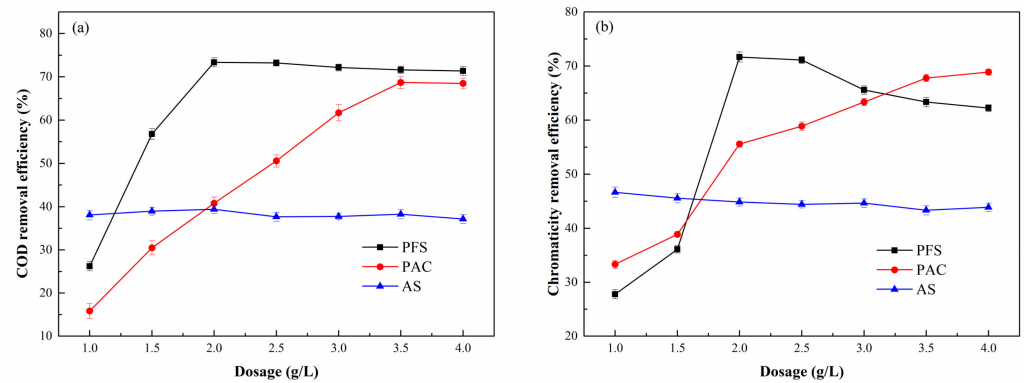


**Figure 2.** Effect of different coagulants and dosages on the removal efficiency of COD (a) and chromaticity (b).

Figure 3 shows the effect of  $\text{pH}_0$  on the removal efficiency of COD and chromaticity when PFS was selected as a coagulant with a dosage of 2 g/L. With the increase in  $\text{pH}_0$ , the treatment efficiency shows a phenomenon of first increasing and then decreasing. When  $\text{pH}_0$  was 6, the removal efficiencies of COD and chromaticity were the highest, at 74.18% and 72.22%, respectively. Since the formation of colloids is easily influenced by pH, too high or too low  $\text{pH}_0$  can adversely affect the coagulation effect [15]. Furthermore, the sludge settling velocity ( $\text{SV}_{30\text{min}}$ ) was 33.8% at a  $\text{pH}_0$  of 6, reflecting a superior sludge sedimentation performance. Therefore, the optimal coagulant was PFS with a dosage of 2 g/L and  $\text{pH}_0$  of 6. The coagulated effluent was used in the subsequent electro- $\text{Fe}^0/\text{H}_2\text{O}_2$  reaction.

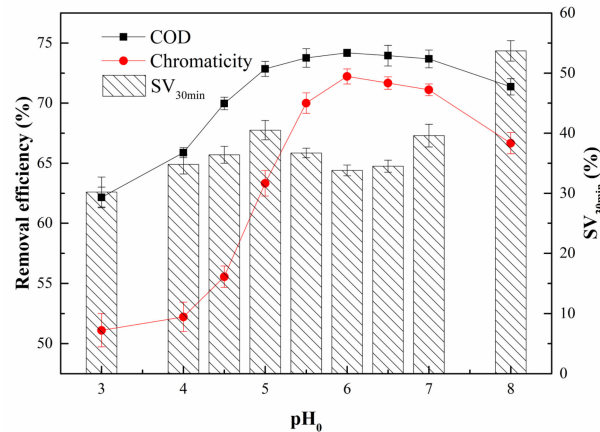


**Figure 3.** The effect of  $\text{pH}_0$  on the removal efficiency when PFS is used as a coagulant.

### 3.2. The Electro- $\text{Fe}^0/\text{H}_2\text{O}_2$ Reaction

#### 3.2.1. Comparison Experiments

In order to evaluate the superiority of the electro- $\text{Fe}^0/\text{H}_2\text{O}_2$  system, the uniform reaction time of 3 h was used to compare the differences in COD and chromaticity removal efficiency between electrochemical oxidation, the  $\text{Fe}^0/\text{H}_2\text{O}_2$  system, and the electro- $\text{Fe}^0/\text{H}_2\text{O}_2$  system. As can be seen from Figure 4, the removal efficiency of COD and chromaticity in leachate by electrochemical oxidation was only 6.79% and 16%, respectively. This is because the hydroxyl radicals generated by electrochemical oxidation were adsorbed on the anode surface and could not effectively degrade the organic matter in the system [23,36]. The removal efficiency of the  $\text{Fe}^0/\text{H}_2\text{O}_2$  system for COD and chromaticity in leachate was 54.12% and 62%, respectively, because in the  $\text{Fe}^0/\text{H}_2\text{O}_2$  system,  $\text{Fe}^{2+}$  is dissolved from the  $\text{Fe}^0$  surface through Equation (3), and the system undergoes the Fenton reaction to produce  $\bullet\text{OH}$ . The hydroxyl radicals, with their extremely high oxidation-reduction

potential ( $E^0 = 2.8$  V), convert the refractory organic compounds into  $\text{CO}_2$ ,  $\text{H}_2\text{O}$ , or a series of intermediates. Additionally, the removal efficiency of the electro- $\text{Fe}^0/\text{H}_2\text{O}_2$  system for COD and chromaticity in leachate was 76.68% and 74%, respectively, because  $\text{Fe}^{3+}$  was reduced to  $\text{Fe}^{2+}$  at the cathode, as shown in Equation (5), which further accelerated the cycle of  $\text{Fe}^{3+}/\text{Fe}^{2+}$  so that more  $\bullet\text{OH}$  was generated in the system and more organic matter was degraded.

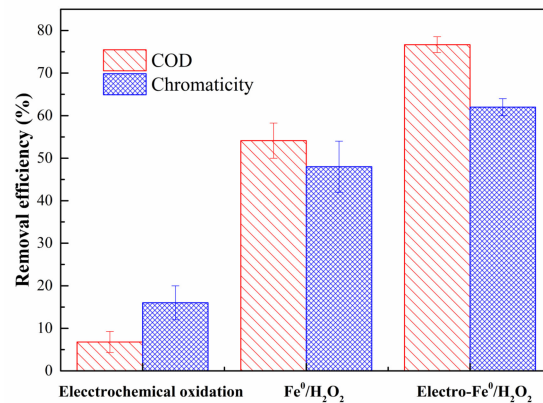


**Figure 4.** Comparison of electrochemical oxidation,  $\text{Fe}^0/\text{H}_2\text{O}_2$ , and electro- $\text{Fe}^0/\text{H}_2\text{O}_2$  for COD and chromaticity removal efficiency from coagulated effluent. Conditions:  $\text{pH}_0 = 3.0$ , current density =  $5 \text{ mA}/\text{cm}^2$ ,  $\text{Fe}^0$  dosage =  $3 \text{ g}/\text{L}$ ,  $\text{H}_2\text{O}_2$  dosage =  $0.059 \text{ M}$ , and reaction time =  $180 \text{ min}$ .

Since COD removal efficiency and chromaticity removal efficiency were positively correlated in the electro- $\text{Fe}^0/\text{H}_2\text{O}_2$  reaction, the COD removal efficiency was used as the study index in the next experiments.

### 3.2.2. Effect of $\text{pH}_0$

One of the most critical factors in the Fenton process is pH. The Fenton process is typically carried out in acidic media. According to most studies, the optimal pH for the Fenton process is around 3 [37]. As can be seen in Figure 5a, the removal efficiency of COD increased from 54.36% to 76.15% when  $\text{pH}_0$  decreased from 5 to 3. Because the  $\text{Fe}^{2+}$  in the system is provided by  $\text{Fe}^0$ , under acidic conditions,  $\text{H}^+$  can corrode the  $\text{Fe}^0$  powder to release  $\text{Fe}^{2+}$ , and  $\text{Fe}^{2+}$  reacts rapidly with hydrogen peroxide to form hydroxyl radicals, as shown in Equation (1). Increased pH in the electro- $\text{Fe}^0/\text{H}_2\text{O}_2$  reaction causes enhanced electro-coagulation via electrostatic attraction or complexation reactions to convert  $\text{Fe}^{2+}$  and  $\text{Fe}^{3+}$  to  $\text{Fe}(\text{OH})_n$ -type structures, weakening the Fenton reaction [37]. While under acidic conditions, the reaction interface on the  $\text{Fe}^0$  surface is maintained, and the generation of iron hydroxide precipitates or hydroxyl complexes is mitigated in the presence of  $\text{H}^+$ , avoiding the coverage of iron oxide on the reaction interface [38]. Furthermore,  $\text{H}_2\text{O}_2$  is relatively stable at pH 3–4; however, when the pH is greater than 4,  $\text{H}_2\text{O}_2$  rapidly decomposes into oxygen and water, causing a decrease in the production of hydroxyl radicals [6]. When the pH was reduced from 3 to 2, the COD removal efficiency decreased from 76.15% to 73.12%. This phenomenon can be attributed to the fact that  $\text{H}_2\text{O}_2$  captured extra  $\text{H}^+$  and produced  $\text{H}_3\text{O}_2^+$ , which inhibited the reaction between  $\text{H}_2\text{O}_2$  and  $\text{Fe}^{2+}$  (Equation (6)) [6].



In addition, coagulation combined with the electro- $\text{Fe}^0/\text{H}_2\text{O}_2$  reaction has distinct advantages. Firstly, the pH of the coagulated effluent is 2.95–3.03, which just meets the optimal pH of the electro- $\text{Fe}^0/\text{H}_2\text{O}_2$  reaction, so there is no need to adjust the pH value separately, thus reducing the cost of chemicals. Next, since the pH value after the reaction was increased to 7.9, aerobic microorganisms could grow well under this condition, which was conducive to the subsequent attainment of the standard treatment. These advantages prove the feasibility of coagulation combined with an electro- $\text{Fe}^0/\text{H}_2\text{O}_2$  reaction.

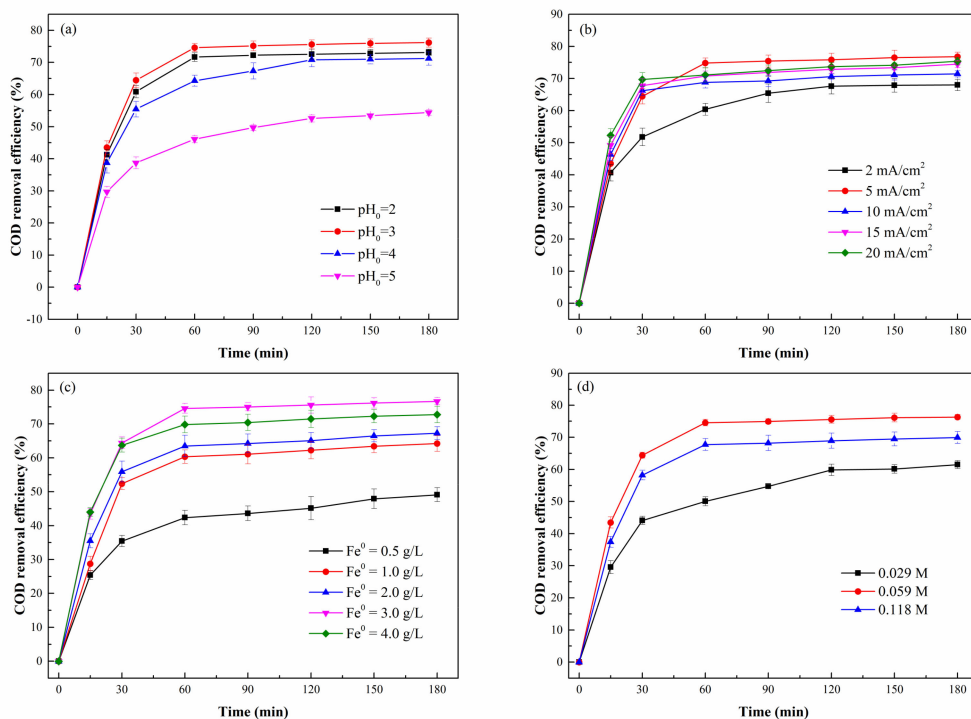


**Figure 5.** Effect of pH<sub>0</sub> (a), current density (b), Fe<sup>0</sup> dosage (c), and H<sub>2</sub>O<sub>2</sub> dosage (d) on COD removal efficiency in the electro-Fe<sup>0</sup>/H<sub>2</sub>O<sub>2</sub> reaction. Except for the investigated parameter, other parameters were controlled as follows: pH<sub>0</sub> = 3.0, current density = 5 mA/cm<sup>2</sup>, Fe<sup>0</sup> dosage = 3 g/L, H<sub>2</sub>O<sub>2</sub> dosage = 0.059 M, and reaction time = 180 min.

### 3.2.3. Effect of Current Density

The effect of current density on the COD removal efficiency of the coagulated effluent was investigated. In general, higher current densities are required to obtain better organic pollutant removal. However, higher current densities may lead to the passivation of the electrode plates and increased energy consumption, resulting in reduced organic contaminant removal performance and higher costs. Therefore, the current density was controlled at 2–20 mA/cm<sup>2</sup>. From Figure 5b, it can be seen that the COD removal efficiency increased from 67.96% to 76.77% when the current density increased from 2 mA/cm<sup>2</sup> to 5 mA/cm<sup>2</sup>, which is because the increase in current density made the regeneration of Fe<sup>2+</sup> through the cathodic reduction reaction faster, as shown in Equation (5), enhancing the efficiency of the Fenton reaction. However, when the current density increased to 10 mA/cm<sup>2</sup>, 15 mA/cm<sup>2</sup>, and 20 mA/cm<sup>2</sup>, the COD removal efficiency decreased compared with that of 5 mA/cm<sup>2</sup>, which was 71.43%, 74.46%, and 75.38%, respectively. Analyzing the reason, when the current density is too high, the oxygen-producing reaction on the anode and the hydrogen-producing reaction on the cathode become dominant (Equations (7) and (8)), leading to a lower COD removal efficiency and inhibiting the regeneration of Fe<sup>2+</sup> [4,20]. Therefore, to maintain the highest and most stable COD removal efficiency, high current densities should not be used. The current density of 2 mA/cm<sup>2</sup> was maintained for the next experiments.



### 3.2.4. Effect of Fe<sup>0</sup> Powder and H<sub>2</sub>O<sub>2</sub> Dosage

The effect of Fe<sup>0</sup> powder dosage on the COD removal efficiency was examined. From Figure 5c, it can be seen that when the amount of Fe<sup>0</sup> powder dosage increased from 0.5 g/L to 3 g/L, the removal efficiency of COD increased from 49.12% to 76.68%, which

is because increasing the amount of  $\text{Fe}^0$  powder caused more  $\text{Fe}^{2+}$  in the solution and accelerated the production of more hydroxyl radicals, as shown in Equation (1). However, the COD removal efficiency decreased to 72.76% with the increase in  $\text{Fe}^0$  powder dosage to 4 g/L. The reason is that when too much  $\text{Fe}^0$  powder is added, excess  $\text{Fe}^{2+}$  is dissolved in the system, and the excess  $\text{Fe}^{2+}$  will compete with organic matter for hydroxyl radicals, resulting in a decrease in COD removal efficiency. The radical scavenging reaction is shown in Equation (9).



In addition, the  $\text{Fe}^{3+}$  produced in the system also increases, and a large amount of  $\text{Fe}(\text{OH})_3$  precipitation adheres to the cathode, resulting in fewer cathode reaction sites and lower  $\text{H}_2\text{O}_2$  production efficiency, resulting in a decrease in COD removal efficiency [39].

It can be seen from Figure 5d that the COD removal efficiency increased from 61.48% to 76.34% when the  $\text{H}_2\text{O}_2$  dosage was increased from 0.029 M to 0.059 M. With the increase in  $\text{H}_2\text{O}_2$  dosage, the production of hydroxyl radicals increased and the oxidation capacity of the system was improved, thus increasing the COD removal efficiency. However, the COD removal efficiency decreased to 69.96% when the  $\text{H}_2\text{O}_2$  dosage was increased to 0.118 M. This is because the excess  $\text{H}_2\text{O}_2$  leads to a scavenging reaction in the system, which produces a relatively low  $\text{HO}_2\bullet$  ( $E^0 = 1.5 \text{ V}$ ), and the  $\text{HO}_2\bullet$  will further consume  $\bullet\text{OH}$ , leading to a decrease in COD removal efficiency (Equations (10) and (11)).



In summary, the dosage of  $\text{Fe}^0$  and  $\text{H}_2\text{O}_2$  were determined to be 3 g/L and 0.059 M.

### 3.3. Organic Matter Conversion and Biodegradability Evaluation

#### 3.3.1. UV-vis Spectra Analysis

The relative amount of organic compounds in wastewater is related to their absorbance in the ultraviolet and visible regions, and the complexity and aromaticity of the organic compounds are related to their absorbance at wavelengths below 380 nm [35]. Therefore, the concentration and molecular degradation of organic matter were evaluated by UV-vis spectra in the coagulation combined with the electro- $\text{Fe}^0/\text{H}_2\text{O}_2$  reaction.

It can be seen from Figure 6 that the leachate still had a high absorbance curve below 380 nm after coagulation, indicating that the coagulated leachate still had high aromaticity and complex organic compounds. After the coagulated effluent was treated by the electro- $\text{Fe}^0/\text{H}_2\text{O}_2$  reaction, the absorbance below the wavelength of 380 nm was greatly reduced, indicating that the electro- $\text{Fe}^0/\text{H}_2\text{O}_2$  reaction has a very good degradation effect on various organic compounds in the coagulated effluent. In addition, the specific absorbance index can reflect the nature of the organic matter in the wastewater. The absorbance at 254 nm ( $E_{254}$ ) and 280 nm ( $E_{280}$ ) represents the relative aromaticity of the organic matter in the leachate, and the greater the values, the higher the aromaticity [27]. In this study, the  $E_{254}$  and  $E_{280}$  of the leachate decreased from 2.0136 and 1.6221 to 0.0894 and 0.0786, respectively, indicating that the aromatic structure of organic matter was largely destroyed after coagulation combined with the electro- $\text{Fe}^0/\text{H}_2\text{O}_2$  reaction. Due to the massive destruction of recalcitrant aromatic compounds, the  $\text{BOD}_5/\text{COD}$  of the leachate improved from 0.049 to 0.46, indicating a significant improvement in the biodegradability of the leachate.

The ratios of  $E_{250}$  to  $E_{365}$  ( $E_{250}/E_{365}$ ) and  $E_{300}$  to  $E_{400}$  ( $E_{300}/E_{400}$ ) represent the molecular weight and the degree of condensation of the organics, respectively [35], with higher ratios indicating lower properties. As shown in Table 2,  $E_{250}/E_{365}$  and  $E_{300}/E_{400}$  showed a small increase after the coagulation process and then a significant increase after the electro- $\text{Fe}^0/\text{H}_2\text{O}_2$  reaction, indicating that the whole process effectively reduced the molecular weight and complexity of the organics.



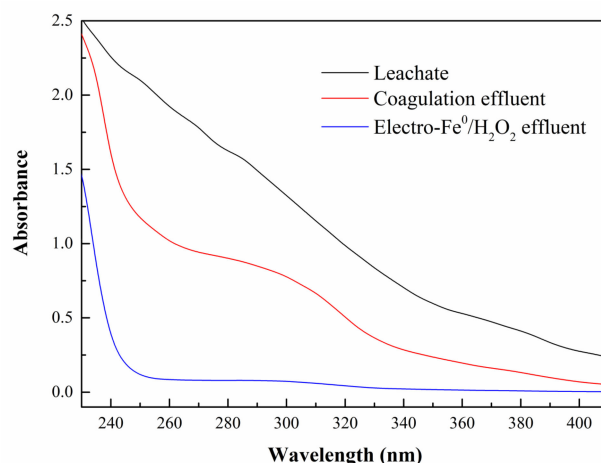


**Figure 6.** The UV-vis spectra of leachate, coagulated effluent, and electro-Fe<sup>0</sup>/H<sub>2</sub>O<sub>2</sub>.

**Table 2.** Special absorbance values for different leachate samples.

Index	Leachate	Coagulated Effluent	Electro-Fe <sup>0</sup> /H <sub>2</sub> O <sub>2</sub> Effluent
E <sub>254</sub>	2.0136	1.0910	0.0894
E <sub>280</sub>	1.6221	0.9026	0.0786
E <sub>250</sub> /E <sub>365</sub>	4.1889	6.6398	9.1463
E <sub>300</sub> /E <sub>400</sub>	4.8279	11.2706	17.6339

### 3.3.2. FRI Analysis of 3D-EEM Spectra

The spectra of the leachate (Figure 7a) showed fluorescence peaks at excitation/emission wavelengths of 240–260/425–475 nm and 300–350/375–475 nm, which all corresponded to humic-like substances and had high fluorescence intensity [40]. In the coagulated effluent spectra (Figure 7b), the fluorescence intensities at excitation/emission wavelengths of 300–350/375–475 nm were reduced, indicating that coagulation can remove part of the humic-like substances. The overall fluorescence intensity of the electro-Fe<sup>0</sup>/H<sub>2</sub>O<sub>2</sub> effluent (Figure 7c) was significantly reduced, indicating that most of the humic-like substances were degraded.

The fluorescence regional integration (FRI) method reveals the configuration of dissolved organic matter (DOM) and is often used to quantitatively analyze the fluorescence intensity data in 3D-EEM [41]. Based on previous research, the EEM spectra are divided into five contiguous regions, namely I, II, III, IV, and V. Regions I, II, III, IV, and V have excitation/emission wavelength ranges of 200–250/260–330 nm, 200–250/330–380 nm, 200–250/380–550 nm, 250–450/260–380 nm, and 250–450/380–550 nm, respectively.

The fluorescence response percentage ( $P_{i,n}$ ) of region  $i$  ( $i = I \sim V$ ) was calculated, as shown in Equations (12)–(14).

$$\Phi_{i,n} = \text{MFi} \times \Phi_i \quad (12)$$

$$\Phi_{T,n} = \sum_{i=1}^5 \Phi_{i,n} \quad (13)$$

$$P_{i,n} = \Phi_{i,n} / \Phi_{T,n} \times 100\% \quad (14)$$

where  $\Phi_i$  is the three-dimensional integration of fluorescence intensity in each region. MFi is the inverse of the ratio of the area of this integral region to the area of the total region.  $\Phi_{i,n}$  is the corrected integrated value of fluorescence intensity.  $\Phi_{T,n}$  is the total corrected cumulative fluorescence intensity of the five regions [41–43].

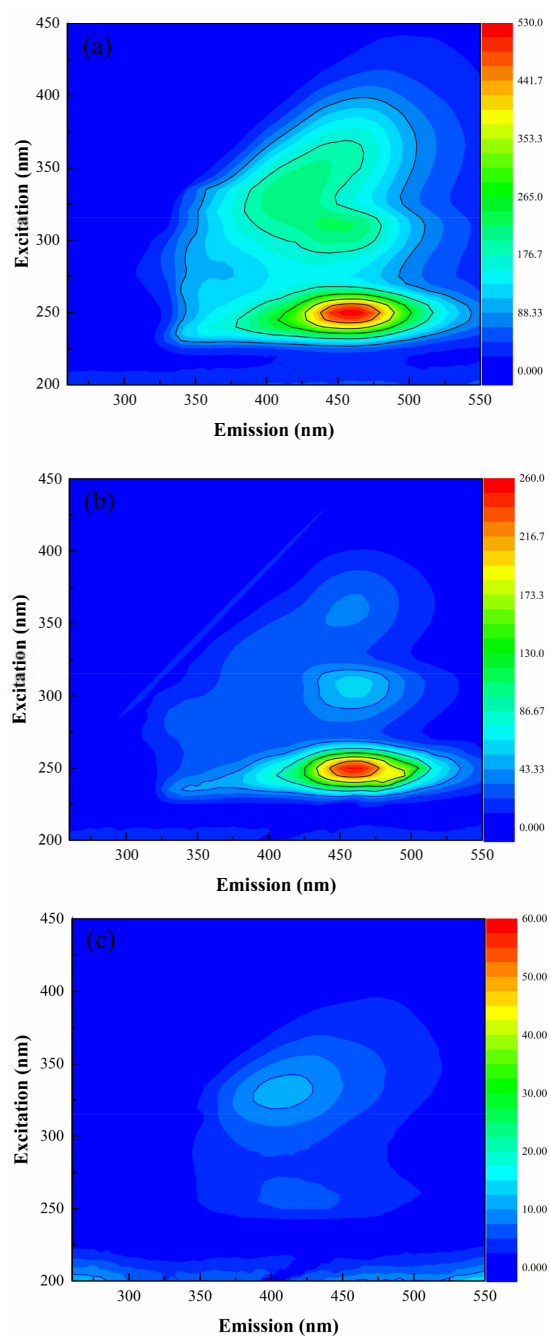


**Figure 7.** The 3D-EEM spectra of leachate (a), coagulated effluent (b), and electro-Fe<sup>0</sup>/H<sub>2</sub>O<sub>2</sub> effluent (c).

Normally, regions I and II are associated with aromatic protein-like substances, and substances in these two regions are easily utilized by microorganisms [5,42]. Region III is associated with fulvic acid-like substances [41]. Region IV is associated with soluble microbial byproduct-like material [5]. Region V is associated with humic acid-like organics [42]. As shown in Figure 8, the  $P_{i,n}$  of regions III and V in the leachate, totaling 63.12%, indicates that the leachate contains a large amount of humic acid and fulvic acid-like substances. After the coagulation process, the  $P_{i,n}$  of region V decreased, and the  $P_{i,n}$  of regions I and II increased, indicating that the coagulation process could remove some humic acid substances. After the electro-Fe<sup>0</sup>/H<sub>2</sub>O<sub>2</sub> reaction, the  $P_{i,n}$  of regions I and II increased to 37.32%, and the  $P_{i,n}$  of regions III and V decreased to 47.58%, indicating that the electro-Fe<sup>0</sup>/H<sub>2</sub>O<sub>2</sub> reaction significantly degraded humic and fulvic acid-like substances in the coagulated effluent, converting them into substances easily used by microorganisms or into CO<sub>2</sub>. This

also proved that the coagulation combined with the electro-Fe<sup>0</sup>/H<sub>2</sub>O<sub>2</sub> reaction improved the biodegradability of the leachate and degraded most humic substances.

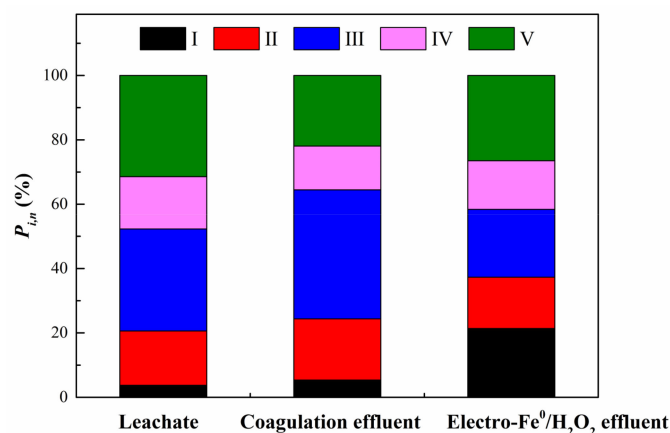


**Figure 8.** The  $P_{i,n}$  values for the DOM of leachate, coagulated effluent, and electro-Fe<sup>0</sup>/H<sub>2</sub>O<sub>2</sub> effluent.

### 3.4. Operating Cost

The operating cost of coagulation combined with the electro-Fe<sup>0</sup>/H<sub>2</sub>O<sub>2</sub> reaction mainly includes the cost of chemicals and electricity. The reagents mainly include PFS, Fe<sup>0</sup> powder, and H<sub>2</sub>O<sub>2</sub>, with prices of 0.12 \$/kg, 0.29 \$/kg, and 0.27 \$/kg, respectively. The dosage of PFS is 2 g/L, and the cost is 0.24 \$/m<sup>3</sup>. The dosage of Fe<sup>0</sup> is 3 g/L, which can be reused, and the loss of Fe<sup>0</sup> is about 0.8 g/L; the cost is 0.23 \$/m<sup>3</sup>. The H<sub>2</sub>O<sub>2</sub> dosage was 0.059 M, and the cost was 0.54 \$/m<sup>3</sup>. The electricity cost, mainly for the DC power supply and electric mixer, was about 3.17 \$/m<sup>3</sup>. The total operating cost was 4.18 \$/m<sup>3</sup>. Compared with the conventional reverse osmosis (8.58 \$/m<sup>3</sup>) [44] and nanofiltration (8.26 \$/m<sup>3</sup>) [45] treatment of landfill leachate, the coagulation combined with the electro-Fe<sup>0</sup>/H<sub>2</sub>O<sub>2</sub> reaction has an obvious cost advantage due to less Fe<sup>0</sup> loss and no pH adjustment. Consequently, the coagulation combined with the electro-Fe<sup>0</sup>/H<sub>2</sub>O<sub>2</sub> reaction is a promising and economically efficient method for the depth treatment of the MBR effluent.

## 4. Conclusions

Coagulation combined with the electro-Fe<sup>0</sup>/H<sub>2</sub>O<sub>2</sub> reaction was developed to treat landfill leachate MBR effluent. After comparison, PFS was considered the best coagulant. When the PFS dosage was 2 g/L and the pH<sub>0</sub> was 6, the removal efficiencies of COD and chromaticity were 74.18% and 72.22%, respectively. Most of the humic-like substances are removed in the coagulation step. The COD and chromaticity removal efficiencies were 76.68% and 74%, respectively, when the coagulated effluent was treated with the electro-Fe<sup>0</sup>/H<sub>2</sub>O<sub>2</sub> reaction under the optimal conditions of pH<sub>0</sub> of 3, a current density of 5 mA/cm<sup>2</sup>, Fe<sup>0</sup> dosage of 3 g/L, and H<sub>2</sub>O<sub>2</sub> dosage of 0.059 M. The reason for the high efficiency of COD and chromaticity removal was that in the electro-Fe<sup>0</sup>/H<sub>2</sub>O<sub>2</sub> system, Fe<sup>3+</sup> could be reduced to Fe<sup>2+</sup> on the surface of Fe<sup>0</sup> powder and on the cathode, which accelerated the cycle between Fe<sup>3+</sup> and Fe<sup>2+</sup> and produced more hydroxyl radicals in the system. In addition, the BOD<sub>5</sub>/COD increased significantly from 0.049 to 0.46, indicating that the biodegradability of the leachate was significantly improved with an operating cost of only 4.18 \$/m<sup>3</sup>. By spectral analysis, humic and fulvic acids were effectively degraded, and the effluent was mostly small molecules of easily biodegradable components. In summary, coagulation combined with the electro-Fe<sup>0</sup>/H<sub>2</sub>O<sub>2</sub> reaction is a promising and cost-effective method for the depth treatment of the MBR effluent and improves biodegradability.

**Author Contributions:** Conceptualization, C.L. and B.Z.; methodology, C.L. and B.Z.; data curation, C.L.; investigation, C.L. and W.L.; resources, W.L. and Q.L.; funding acquisition, B.Z.; supervision, B.Z.; writing—original draft, C.L.; writing—review & editing, C.L. and B.Z. All authors have read and agreed to the published version of the manuscript.

**Funding:** This research was funded by the Foshan Science and Technology Innovation Project of Guangdong Province (No. 2130218003140).

**Data Availability Statement:** The data presented in this study are available on request from the corresponding author. The data are not publicly available to avoid possible misuse or unauthorized use of them.

**Conflicts of Interest:** The authors declare no conflict of interest.

## References

1. Li, M.; Zhou, M.; Qin, X. A feasible electro-Fenton treatment of landfill leachate diluted by electro-Fenton effluent: Evaluation of operational parameters, effect of dilution ratio and assessment of treatment cost. *J. Water Process Eng.* **2022**, *47*, 102754. [[CrossRef](#)]
2. Teng, C.; Zhou, K.; Peng, C.; Chen, W. Characterization and treatment of landfill leachate: A review. *Water Res.* **2021**, *203*, 117525. [[CrossRef](#)] [[PubMed](#)]
3. Moradian, F.; Ramavandi, B.; Jaafarzadeh, N.; Kouhgard, E. Effective treatment of high-salinity landfill leachate using ultraviolet/ultrasonication/ peroxymonosulfate system. *Waste Manag.* **2020**, *118*, 591–599. [[CrossRef](#)] [[PubMed](#)]
4. Fernandes, A.; Pacheco, M.J.; Ciriaco, L.; Lopes, A. Review on the electrochemical processes for the treatment of sanitary landfill leachates: Present and future. *Appl. Catal. B Environ.* **2015**, *176–177*, 183–200. [[CrossRef](#)]
5. Deng, Y.; Feng, C.; Chen, N.; Hu, W.; Kuang, P.; Liu, H.; Hu, Z.; Li, R. Research on the treatment of biologically treated landfill leachate by joint electrochemical system. *Waste Manag.* **2018**, *82*, 177–187. [[CrossRef](#)]
6. Fang, Y.; Yin, W.; Jiang, Y.; Ge, H.; Li, P.; Wu, J. Depth treatment of coal-chemical engineering wastewater by a cost-effective sequential heterogeneous Fenton and biodegradation process. *Environ. Sci. Pollut. Res. Int.* **2018**, *25*, 13118–13126. [[CrossRef](#)]
7. Liu, J.; Zhang, P.; Tian, Z.; Xu, R.; Wu, Y.; Song, Y. Pollutant removal from landfill leachate via two-stage anoxic/oxic combined membrane bioreactor: Insight in organic characteristics and predictive function analysis of nitrogen-removal bacteria. *Bioresour. Technol.* **2020**, *317*, 124037. [[CrossRef](#)]
8. Ahmed, F.N.; Lan, C.Q. Treatment of landfill leachate using membrane bioreactors: A review. *Desalination* **2012**, *287*, 41–54. [[CrossRef](#)]
9. Amor, C.; Torres-Socias, E.D.; Peres, J.A.; Maldonado, M.I.; Oller, I.; Malato, S.; Lucas, M.S. Mature landfill leachate treatment by coagulation/flocculation combined with Fenton and solar photo-Fenton processes. *J. Hazard. Mater.* **2015**, *286*, 261–268. [[CrossRef](#)]
10. Kurniawan, T.A.; Lo, W.H.; Chan, G.Y. Degradation of recalcitrant compounds from stabilized landfill leachate using a combination of ozone-GAC adsorption treatment. *J. Hazard. Mater.* **2006**, *137*, 443–455. [[CrossRef](#)]
11. Xu, Q.; Siracusa, G.; Di Gregorio, S.; Yuan, Q. COD removal from biologically stabilized landfill leachate using Advanced Oxidation Processes (AOPs). *Process Saf. Environ. Prot.* **2018**, *120*, 278–285. [[CrossRef](#)]
12. Wang, G.; Fan, Z.; Wu, D.; Qin, L.; Zhang, G.; Gao, C.; Meng, Q. Anoxic/aerobic granular active carbon assisted MBR integrated with nanofiltration and reverse osmosis for advanced treatment of municipal landfill leachate. *Desalination* **2014**, *349*, 136–144. [[CrossRef](#)]
13. Bogacki, J.; Marcinowski, P.; El-Khozondar, B. Treatment of Landfill Leachates with Combined Acidification/Coagulation and The Fe<sup>0</sup>/H<sub>2</sub>O<sub>2</sub> Process. *Water* **2019**, *11*, 194. [[CrossRef](#)]
14. Yusoff, M.S.; Aziz, H.A.; Zamri, M.; Suja, F.; Abdullah, A.Z.; Basri, N.E.A. Floc behavior and removal mechanisms of cross-linked Durio zibethinus seed starch as a natural flocculant for landfill leachate coagulation-flocculation treatment. *Waste Manag.* **2018**, *74*, 362–372. [[CrossRef](#)]
15. Chen, W.; Gu, Z.; Wen, P.; Li, Q. Degradation of refractory organic contaminants in membrane concentrates from landfill leachate by a combined coagulation-ozonation process. *Chemosphere* **2019**, *217*, 411–422. [[CrossRef](#)]
16. Deng, Y.; Englehardt, J.D. Treatment of landfill leachate by the Fenton process. *Water Res.* **2006**, *40*, 3683–3694. [[CrossRef](#)]
17. da Costa, F.M.; Daflon, S.D.A.; Bila, D.M.; da Fonseca, F.V.; Campos, J.C. Evaluation of the biodegradability and toxicity of landfill leachates after pretreatment using advanced oxidative processes. *Waste Manag.* **2018**, *76*, 606–613. [[CrossRef](#)]
18. Wang, X.; Chen, S.; Gu, X.; Wang, K. Pilot study on the advanced treatment of landfill leachate using a combined coagulation, fenton oxidation and biological aerated filter process. *Waste Manag.* **2009**, *29*, 1354–1358. [[CrossRef](#)]
19. Jurczyk, L.; Koc-Jurczyk, J. Quantitative dynamics of ammonia-oxidizers during biological stabilization of municipal landfill leachate pretreated by Fenton's reagent at neutral pH. *Waste Manag.* **2017**, *63*, 310–326. [[CrossRef](#)]
20. Zhang, H.; Zhang, D.; Zhou, J. Removal of COD from landfill leachate by electro-Fenton method. *J. Hazard. Mater.* **2006**, *135*, 106–111. [[CrossRef](#)]
21. Kallel, M.; Belaid, C.; Mechichi, T.; Ksibi, M.; Elleuch, B. Removal of organic load and phenolic compounds from olive mill wastewater by Fenton oxidation with zero-valent iron. *Chem. Eng. J.* **2009**, *150*, 391–395. [[CrossRef](#)]
22. Martins, R.C.; Lopes, D.V.; Quina, M.J.; Quinta-Ferreira, R.M. Treatment improvement of urban landfill leachates by Fenton-like process using ZVI. *Chem. Eng. J.* **2012**, *192*, 219–225. [[CrossRef](#)]
23. Wang, Z.; Li, J.; Tan, W.; Wu, X.; Lin, H.; Zhang, H. Removal of COD from landfill leachate by advanced Fenton process combined with electrolysis. *Sep. Purif. Technol.* **2019**, *208*, 3–11. [[CrossRef](#)]

24. Qiang, Z.; Chang, J.-H.; Huang, C.-P. Electrochemical regeneration of  $\text{Fe}_{2+}$  in Fenton oxidation processes. *Water Res.* **2003**, *37*, 1308–1319. [[CrossRef](#)] [[PubMed](#)]
25. Ding, J.; Jiang, M.; Zhao, G.; Wei, L.; Wang, S.; Zhao, Q. Treatment of leachate concentrate by electrocoagulation coupled with electro-Fenton-like process: Efficacy and mechanism. *Sep. Purif. Technol.* **2021**, *255*, 117668. [[CrossRef](#)]
26. Liang, L.; Cheng, L.; Zhang, Y.; Wang, Q.; Wu, Q.; Xue, Y.; Meng, X. Efficiency and mechanisms of rhodamine B degradation in Fenton-like systems based on zero-valent iron. *RSC Adv.* **2020**, *10*, 28509–28515. [[CrossRef](#)]
27. Chen, W.; Zhang, A.; Gu, Z.; Li, Q. Enhanced degradation of refractory organics in concentrated landfill leachate by  $\text{Fe}_0/\text{H}_2\text{O}_2$  coupled with microwave irradiation. *Chem. Eng. J.* **2018**, *354*, 680–691. [[CrossRef](#)]
28. Deng, Y.; Englehardt, J.D. Kinetics and oxidative mechanism for  $\text{H}_2\text{O}_2$ -enhanced iron-mediated aeration (IMA) treatment of recalcitrant organic compounds in mature landfill leachate. *J. Hazard. Mater.* **2009**, *169*, 370–375. [[CrossRef](#)]
29. Bu, Z.; Li, X.; Xue, Y.; Ye, J.; Zhang, J.; Pan, Y. Hydroxylamine enhanced treatment of highly salty wastewater in  $\text{Fe}_0/\text{H}_2\text{O}_2$  system: Efficiency and mechanism study. *Sep. Purif. Technol.* **2021**, *271*, 118847. [[CrossRef](#)]
30. Bremner, D.H.; Burgess, A.E.; Houlemare, D.; Namkung, K.-C. Phenol degradation using hydroxyl radicals generated from zero-valent iron and hydrogen peroxide. *Appl. Catal. B Environ.* **2006**, *63*, 15–19. [[CrossRef](#)]
31. Brillas, E.; Sirés, I.; Oturan, M.A. Electro-Fenton process and related electrochemical technologies based on Fenton's reaction chemistry. *Chem. Rev.* **2009**, *109*, 6570–6631. [[CrossRef](#)]
32. Kayan, B.; Gozmen, B.; Demirel, M.; Gizir, A.M. Degradation of acid red 97 dye in aqueous medium using wet oxidation and electro-Fenton techniques. *J. Hazard. Mater.* **2010**, *177*, 95–102. [[CrossRef](#)]
33. Kocanova, V.; Dusek, L. Electrochemical dissolution of steel as a typical catalyst for electro-Fenton oxidation. *Mon. Chem.* **2016**, *147*, 935–941. [[CrossRef](#)]
34. Apha, A. *WEF (2005) Standard Methods for the Examination of Water and Wastewater*; National Government Publication: Washington, DC, USA, 2007; Available online: <https://www.worldcat.org> (accessed on 28 June 2022).
35. Wang, F.; Luo, Y.; Ran, G.; Li, Q. Sequential coagulation and  $\text{Fe}(0)\text{-O}_3/\text{H}_2\text{O}_2$  process for removing recalcitrant organics from semi-aerobic aged refuse biofilter leachate: Treatment efficiency and degradation mechanism. *Sci. Total. Environ.* **2020**, *699*, 134371. [[CrossRef](#)]
36. Mandal, P.; Dubey, B.K.; Gupta, A.K. Review on landfill leachate treatment by electrochemical oxidation: Drawbacks, challenges and future scope. *Waste Manag.* **2017**, *69*, 250–273. [[CrossRef](#)]
37. Nidheesh, P.V.; Gandhimathi, R. Trends in electro-Fenton process for water and wastewater treatment: An overview. *Desalination* **2012**, *299*, 1–15. [[CrossRef](#)]
38. Yun, W.K.; Hwang, K.Y. Effects of reaction conditions on the oxidation efficiency in the Fenton process. *Water Res.* **2000**, *34*, 2786–2790.
39. Wang, Y.; Li, X.; Zhen, L.; Zhang, H.; Zhang, Y.; Wang, C. Electro-Fenton treatment of concentrates generated in nanofiltration of biologically pretreated landfill leachate. *J. Hazard. Mater.* **2012**, *229–230*, 115–121. [[CrossRef](#)]
40. Stedmon, C.A.; Markager, S.; Bro, R. Tracing dissolved organic matter in aquatic environments using a new approach to fluorescence spectroscopy. *Mar. Chem.* **2003**, *82*, 239–254. [[CrossRef](#)]
41. He, X.S.; Xi, B.D.; Wei, Z.M.; Jiang, Y.H.; Yang, Y.; An, D.; Cao, J.L.; Liu, H.L. Fluorescence excitation-emission matrix spectroscopy with regional integration analysis for characterizing composition and transformation of dissolved organic matter in landfill leachates. *J. Hazard. Mater.* **2011**, *190*, 293–299. [[CrossRef](#)]
42. Wen, C.; Paul, W.; Leenheer, J.A.; Karl, B. Fluorescence excitation-emission matrix regional integration to quantify spectra for dissolved organic matter. *Environ. Sci. Technol.* **2003**, *37*, 5701–5710.
43. He, X.S.; Xi, B.D.; Li, X.; Pan, H.W.; An, D.; Bai, S.G.; Li, D.; Cui, D.Y. Fluorescence excitation-emission matrix spectra coupled with parallel factor and regional integration analysis to characterize organic matter humification. *Chemosphere* **2013**, *93*, 2208–2215. [[CrossRef](#)] [[PubMed](#)]
44. de Almeida, R.; Bila, D.M.; Quintaes, B.R.; Campos, J.C. Cost estimation of landfill leachate treatment by reverse osmosis in a Brazilian landfill. *Waste Manag. Res.* **2020**, *38*, 1087–1092. [[CrossRef](#)] [[PubMed](#)]
45. de Almeida, R.; de Souza Couto, J.M.; Gouvea, R.M.; de Almeida Oroski, F.; Bila, D.M.; Quintaes, B.R.; Campos, J.C. Nanofiltration applied to the landfill leachate treatment and preliminary cost estimation. *Waste Manag. Res.* **2020**, *38*, 1119–1128. [[CrossRef](#)]

**Disclaimer/Publisher's Note:** The statements, opinions and data contained in all publications are solely those of the individual author(s) and contributor(s) and not of MDPI and/or the editor(s). MDPI and/or the editor(s) disclaim responsibility for any injury to people or property resulting from any ideas, methods, instructions or products referred to in the content.